



A multi-direction virtual array transformation algorithm for 2D DOA estimation

Kai-jie Xu^a, Wei-ke Nie^{a,*}, Da-zheng Feng^b, Xiao-jiang Chen^a, Ding-yi Fang^a

^a School of Information Science and Technology, Northwest University, Xi'an 710127, China

^b National Lab of Radar Signal Processing, Xidian University, Xi'an 710071, China

ARTICLE INFO

Article history:

Received 20 June 2015

Received in revised form

31 December 2015

Accepted 4 January 2016

Available online 29 January 2016

Keywords:

2D DOA

Array signal processing

Virtual transformation

Real and virtual subspaces

ABSTRACT

In this paper, a multi-direction virtual array transformation algorithm termed MVATA for two dimension (2D) direction of arrival (DOA) estimation is proposed. A kind of multi-direction rotation invariant virtual subarrays is firstly constructed. Secondly, by singular value decomposition (SVD) of the response matrix of the real array to signals from a sector, the interpolation matrices can be estimated and from which the real and virtual signal subspaces are further estimated. Thirdly, a rotational invariant factor matrix is derived from the real and virtual subspaces base on least squares. Subsequently, the azimuth and elevation can be solved through the rotational invariant factor matrix without spectral peak search. Theoretical calculation and time-consuming statistics show that the proposed MVATA has the advantage of computational complexity compared with the conventional interpolated methods. Moreover, the proposed MVATA can be applied to arbitrary structure array, and the estimated 2D angles can be paired automatically. Simulation results demonstrate the proposed MVATA possesses significantly accuracy improvement especially in low SNR and small snapshots.

© 2016 Elsevier B.V. All rights reserved.

1. Introduction

DOA estimation is the key technology in radar, sonar, mobile communication and so on. During its development, one dimensional (1D) estimation has been widely investigated [1]. Two of its most important representatives are MUSIC [2] and ESPRIT [3], which are both categorized as eigen decomposition based methods. MUSIC algorithm is well-known for its high resolution capability. It can be applied in arbitrary array manifold to estimate multiple parameters of each source. However, MUSIC algorithm must know the analytical relation of its array response matrix to all possible combinations of source parameters. The ESPRIT algorithm, without spectral peak search and complex computation, has been considered to be a very

extensive application value algorithm since it yields. Its principal advantage is that the DOA parameters are obtained with a closed form solution.

At first, ESPRIT algorithm can only be applied to uniform linear array (ULA) for 1D DOA estimation, while 2D estimation is of greater practical importance. ESPRIT algorithm cannot be directly used to uniform circular array (UCA) or arbitrary array. However, its application reduces the effective array aperture, usually it needs to pair the parameters in 2D estimation [4]. In 2D scenario, MUSIC algorithm costs a majority of run time during the procedure of space spectrum peak search.

Recently, virtual array transformation technology [5] has improved the applicability of 2D ESPRIT algorithms and can be applied in arbitrary array manifold. Usually, there are three ways to implement virtual array transformation, i.e. array interpolation [6], higher-order cumulant [7] and extrapolation algorithm [8]. However, higher-order cumulant is suffered from large amount of computation complex [9], and

* Corresponding author. Tel.: +86 13891933536.

E-mail address: weikenie@163.com (W.-k. Nie).

extrapolation algorithm can not distinguish two targets when they are relatively close each other. Array interpolation method is proposed by Bronez [10] firstly and later in different formulations by Friedlander [11]. Most of these methods can be directly applied to arbitrary array [12]. In [13] a single direction virtual interpolation algorithm termed TVIA was proposed via two virtual subarrays. TVIA uses the virtual interpolation technology twice to get the rotational invariance factor, from which the elevation angle can be estimated via rotational invariance technique. Then the estimated elevation angle is substituted into the real array manifold, hence the azimuth angle is obtained by one dimensional search. TVIA achieves higher DOA estimation accuracy than the well-known algorithm proposed by Bronez [11], and it can be applied to arbitrary array, meanwhile the estimated elevation and azimuth can be automatically paired. However, TVIA still needs 1D spectrum peak search which leads to the high computation and storage costs, at the same time it cannot distinguish signals with the same elevation but different azimuths. In [14], Yang proposed a novel 2D DOA finding algorithm for arbitrary array applications. He decomposes the 2D problem into two 1D problems by 2D DFT beam space ESPRIT algorithm, and the estimated 2D angle need to be paired.

In this paper, we propose a novel multi-direction virtual array transformation algorithm (MVATA) for 2D DOA estimation, which can effectively solve the existing problems of traditional virtual array transformation algorithms. The theoretical derivation and simulation results of the algorithm are given. Compared with the TVIA for 2D DOA estimation, the proposed MVATA has the following advantages. (1) It does not need spectrum peak search and fractal dimension processing, hence the computation and storage costs can be reduced efficiently. (2) As the azimuth and its corresponding elevation angle are obtained from the same element of a diagonal matrix, they need not the support of pairing algorithm. (3) The accuracy of the 2D DOA estimation is obviously improved especially in the scenarios of low SNR and small snapshots. (4) Two dimension angels which have the same azimuth or elevation angle can also be distinguished. The proposed algorithm can be applied not only to UCA but also to arbitrary structure arrays. Simulation results demonstrate its effectiveness.

2. Signal model and approach of TVIA

2.1. Signal model

Consider a UCA composed of M elements impinged by P narrowband signals $s_p(t)$ $p = 1, 2, \dots, P$, where t is the time variable. The distance between the neighboring elements is no greater than half the wavelength. As shown in Fig. 1, the coordinate of the m th ($m = 1, 2, \dots, M$) element in the Cartesian coordinate system is $\mathbf{p}_m = [x_m, y_m, z_m]^T$. The P sources are assumed as far field with azimuth α_p and elevation β_p , $p = 1, 2, \dots, P$. Assume the radius of UCA is R and the noise is Gaussian white noise. From Fig. 1, we know the DOA unit vector of source is

$$\mathbf{d}_p = [\cos \alpha_p \sin \beta_p \quad \sin \alpha_p \sin \beta_p \quad \cos \beta_p]^T \quad (1)$$

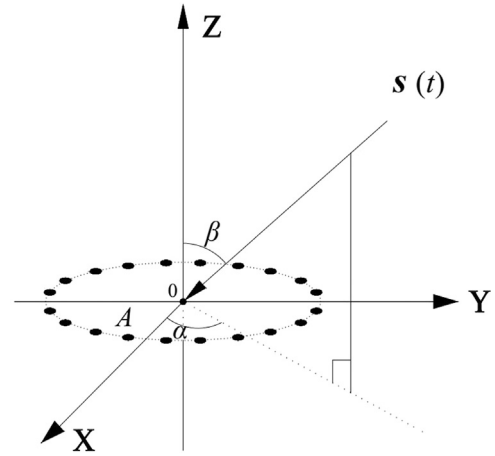


Fig. 1. The coordinates system of UCA.

when the m th array receives the data of the p th source, the wave path difference is given by

$$\Delta_{mp}(\alpha_p, \beta_p) = \mathbf{p}_m^T \mathbf{d}_p \quad (2)$$

Hence the complex factor corresponding to phase difference can be expressed as

$$a_{mp}(\alpha_p, \beta_p) = \exp[-j(2\pi/\lambda)\Delta_{mp}(\alpha_p, \beta_p)] \quad (3)$$

Furthermore, for UCA, substituting (2) into (3), Eq. (3) can be changed as

$$a_{mp}(\alpha_p, \beta_p) = \exp\{-j(2\pi/\lambda)R \sin \beta_p \cos [2\pi(m-1)/M - \alpha_p]\} \quad (4)$$

The ideal steering matrix for UCA array is

$$\mathbf{A} = [\mathbf{a}(\alpha_1, \beta_1) \quad \mathbf{a}(\alpha_2, \beta_2) \quad \dots \quad \mathbf{a}(\alpha_P, \beta_P)] \quad (5)$$

$$\mathbf{a}(\alpha_p, \beta_p) = [a_{1p}(\alpha_p, \beta_p) \quad \dots \quad a_{mp}(\alpha_p, \beta_p) \quad \dots \quad a_{Mp}(\alpha_p, \beta_p)]^T \quad (6)$$

where $m = 1, 2, \dots, M$, $p = 1, 2, \dots, P$, λ is the wavelength of the signal. Let the $M \times 1$ observed array received data of the t th snapshot be $\mathbf{x}(t)$, which can be written as

$$\mathbf{x}(t) = \sum_{p=1}^P \mathbf{a}(\alpha_p, \beta_p) s_p(t) + \mathbf{n}(t) \quad t = t_1, t_2, \dots, t_{N_s} \quad (7)$$

Eq. (7) can be written in matrix form as

$$\mathbf{X} = \mathbf{A}\mathbf{S} + \mathbf{N} \quad \text{with} \quad \begin{cases} \mathbf{X} = [\mathbf{x}(t_1), \mathbf{x}(t_2), \dots, \mathbf{x}(t_{N_s})] \\ \mathbf{S} = [\mathbf{s}(t_1), \mathbf{s}(t_2), \dots, \mathbf{s}(t_{N_s})] \\ \mathbf{N} = [\mathbf{n}(t_1), \mathbf{n}(t_2), \dots, \mathbf{n}(t_{N_s})] \end{cases} \quad (8)$$

2.2. Previous approaches (TVIA)

Here we directly summarized the procedure of TVIA as follows:

- Step 1: The array covariance matrix of received vector $\mathbf{x}(t)$ is

$$\mathbf{R}_{\mathbf{xx}}(t) = E[\mathbf{x}(t)\mathbf{x}(t)^H] = \mathbf{A}\mathbf{R}_{\mathbf{ss}}\mathbf{A}^H + \sigma^2\mathbf{I} \quad (9)$$

where $\mathbf{R}_{\mathbf{ss}} = E[\mathbf{s}(t)\mathbf{s}(t)^H]$ is the full rank sources covariance matrix, $\mathbf{s}(t) = [s_1(t), s_2(t), \dots, s_P(t)]^T$ is the vector of source waveforms, σ^2 is noise power, \mathbf{I} is $M \times M$ identity matrix. $E[\bullet]$ and $[\bullet]^H$ denote the statistical expectation and the Hermitian transpose, respectively. The estimated covariance matrix $\hat{\mathbf{R}}_{\mathbf{xx}}$ of received data matrix \mathbf{X} can be derived from a set of sample snapshots as

$$\hat{\mathbf{R}}_{\mathbf{xx}} = \frac{1}{N_S} \sum_{i=1}^{N_S} \mathbf{x}(t_i)\mathbf{x}(t_i)^H = \frac{1}{N_S} \mathbf{X}\mathbf{X}^H \quad (10)$$

where N_S is the total number of snapshots. Then the eigen decomposition of $\hat{\mathbf{R}}_{\mathbf{xx}}$ is

$$\hat{\mathbf{R}}_{\mathbf{xx}} = \mathbf{U}\mathbf{\Sigma}\mathbf{U}^H = \sum_{i=1}^M \varepsilon_i \mathbf{v}_i \mathbf{v}_i^H \quad (11)$$

where $\mathbf{\Sigma} = \text{diag}\{\varepsilon_1 \geq \varepsilon_2 \geq \dots \geq \varepsilon_M\}$, ε_i and \mathbf{v}_i are the eigenvalue and corresponding eigenvector of $\hat{\mathbf{R}}_{\mathbf{xx}}$ respectively. In ideal conditions, we have relation $\varepsilon_1 \geq \varepsilon_2 \geq \dots \geq \varepsilon_P \geq \varepsilon_{P+1} = \dots = \varepsilon_M = \sigma^2$. If the number of signals has been estimated by MDL criterion [15], $\hat{\mathbf{R}}_{\mathbf{xx}}$ can be decomposed as

$$\hat{\mathbf{R}}_{\mathbf{xx}} = \mathbf{U}_S \mathbf{\Sigma}_S \mathbf{U}_S^H + \mathbf{U}_N \mathbf{\Sigma}_N \mathbf{U}_N^H \quad (12)$$

where $\mathbf{U}_S = [\mathbf{v}_1, \mathbf{v}_2, \dots, \mathbf{v}_P]$ and $\mathbf{U}_N = [\mathbf{v}_{P+1}, \mathbf{v}_{P+2}, \dots, \mathbf{v}_M]$ are the signal subspace and noise subspace respectively.

- Step 2: Virtual arrays \mathbf{A}' and \mathbf{A}'' can be constructed via interpolation technique, as shown in Fig. 2. The real array and virtual array are expressed as the solid circle and hollow circle, \mathbf{A}' and \mathbf{A}'' are the steering matrices of UCAs with different altitude, such that \mathbf{A} , \mathbf{A}' and \mathbf{A}'' are associated to the altitude 0, d and $2d$ respectively. So the signal subspace of the virtual array \mathbf{U}'_S and \mathbf{U}''_S can be obtained by

$$\begin{aligned} \mathbf{U}'_S &\approx \mathbf{B}'_k \mathbf{U}_S \\ \mathbf{U}''_S &\approx \mathbf{B}''_k \mathbf{U}_S \end{aligned} \quad (13)$$

where \mathbf{B}'_k and \mathbf{B}''_k are the interpolation matrices of [13].

- Step 3: Obtain the eigenvalues φ_p , $p = 1, 2, \dots, P$ of the matrix $(\mathbf{U}_S^H \mathbf{U}'_S)^{-1} \mathbf{U}_S^H \mathbf{U}''_S$, the ESPRIT algorithm can be

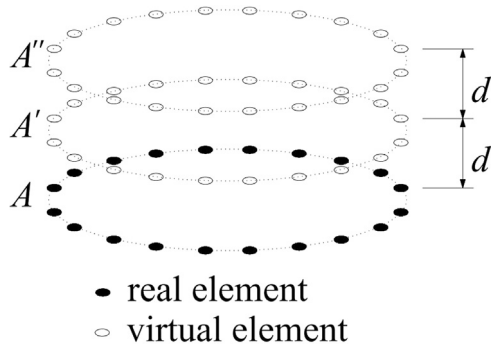


Fig. 2. Array configuration of TVIA.

used to estimate the elevation angle β_p as

$$\beta_p = \arccos \left[\frac{\lambda \text{angle}(\varphi_p)}{2\pi d} \right] \quad (14)$$

- Step 4: The azimuth angle α_p can be obtained by the spectrum peak search with MUSIC algorithm.

3. Principle of the proposed algorithm (MVATA)

For simplicity, we illustrate our proposed algorithm based on the array model above. Assume there is a signal, whose elevation is in the sector $\Theta_\beta \in [\theta_{\beta l}, \theta_{\beta r}]$, and its azimuth is in the sector $\Theta_\alpha \in [\theta_{\alpha l}, \theta_{\alpha r}]$. Let $\Delta\theta$ be the interpolation step, then Θ_β and Θ_α can be discretized as

$$\begin{aligned} \Theta_\beta &= \{\beta_i = \theta_{\beta l} + (i-1)\Delta\theta \mid 1 \leq i \leq I, \beta_i \leq \theta_{\beta r}\} \\ \Theta_\alpha &= \{\alpha_j = \theta_{\alpha l} + (j-1)\Delta\theta \mid 1 \leq j \leq J, \alpha_j \leq \theta_{\alpha r}\} \end{aligned} \quad (15)$$

In the sector, the real array manifold is

$$\begin{aligned} \mathbf{A}_f &= \begin{bmatrix} \dots & \mathbf{a}_f(\alpha_j, \beta_i) & \dots \end{bmatrix} \quad \alpha_j \in \Theta_\alpha \quad (1 \leq j \leq J), \\ \beta_i &\in \Theta_\beta \quad (1 \leq i \leq I) \end{aligned} \quad (16)$$

In other words, \mathbf{A}_f is a M rows and $J \times I$ columns matrix. It is the response of the real array to signals, and the interpolation numbers J and I are determined by the desired accuracy. In this paper we extend two virtual arrays via interpolation technique, as shown in Fig. 3, where δ_1 and δ_2 are the direction angles of the two interpolated virtual arrays. Without loss of generality, we let $\delta_1 = \delta_2 = \delta$ in this paper, therefore, the coordinate of the virtual elements P'_m and P''_m , $m = 1, 2, \dots, M$ in the rectangular coordinate system are $(x_m, y_m + d \cos \delta, z_m + d \sin \delta)$ and $(x_m, y_m + d \cos \delta, z_m - d \sin \delta)$. The steering matrices \mathbf{A}' and \mathbf{A}'' in the same sector with Omni-direction radiation pattern

$$\begin{aligned} \mathbf{A}' &= \begin{bmatrix} \dots & \mathbf{a}'(\alpha_j, \beta_i) & \dots \end{bmatrix} \\ \mathbf{A}'' &= \begin{bmatrix} \dots & \mathbf{a}''(\alpha_j, \beta_i) & \dots \end{bmatrix} \end{aligned} \quad \alpha_j \in \Theta_\alpha \quad (1 \leq j \leq J), \beta_i \in \Theta_\beta \quad (1 \leq i \leq I) \quad (17)$$

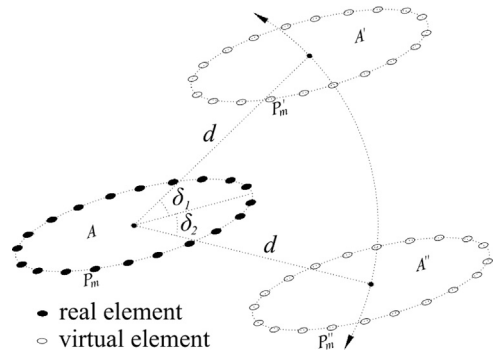


Fig. 3. Array configuration of proposed MVATA.

Table 1
Computational complexity of the TVIA.

Estimate the elevation by ESPRIT	MDN
a) $\mathbf{R}_{\mathbf{X}\mathbf{X}} = E[\mathbf{X}\mathbf{X}^H]$	$M^2 N_S + 1$
b) $\mathbf{R}_{\mathbf{X}\mathbf{X}} = \mathbf{U}\mathbf{\Sigma}\mathbf{U}^H$	$M^3 + 2M^2$
c) $\mathbf{U}'_S \approx \mathbf{B}'_k \mathbf{U}_S$	$M^2 P$
d) $\mathbf{U}'_S \approx \mathbf{B}'_k \mathbf{U}_S$	$M^2 P$
e) $(\mathbf{U}_S^H \mathbf{U}_S)^{-1} \mathbf{U}_S^H \mathbf{U}'_S$	$MP^2 + \frac{2}{3}P^3 + 2MP^2$
f) $\text{SVD}[(\mathbf{U}_S^H \mathbf{U}_S)^{-1} \mathbf{U}_S^H \mathbf{U}'_S]$	$P^3 + 2P^2$
g) $\beta_p = \arccos\left[\frac{\angle(\mathbf{a}_p)}{2\pi d}\right]$	$4P$
Search the azimuth by MUSIC	
h) $P_{\text{MUSIC}} = \frac{1}{\mathbf{a}^H(\beta_p, \alpha_1) \mathbf{U}_N \mathbf{U}_N^H \mathbf{a}(\beta_p, \alpha_1)}$	$\Gamma(M^2 + 9M) + M^2(M - P)$ ($\Gamma > M$)
Total MDN	
$M^2(N_S) + 1 + M^3 + 2M^2 + M^2P + M^2P + MP^2 + \frac{2}{3}P^3 + 2MP^2 + P^3 + 2P^2 + 4P + \Gamma(M^2 + 9M) + M^2(M - P)$	
$= \Gamma(M^2 + 9M) + 2M^3 + (N_S + 2P + 2)M^2 + 2P^2M + \frac{5}{3}P^3 + 2P^2 + 4P + 1$	

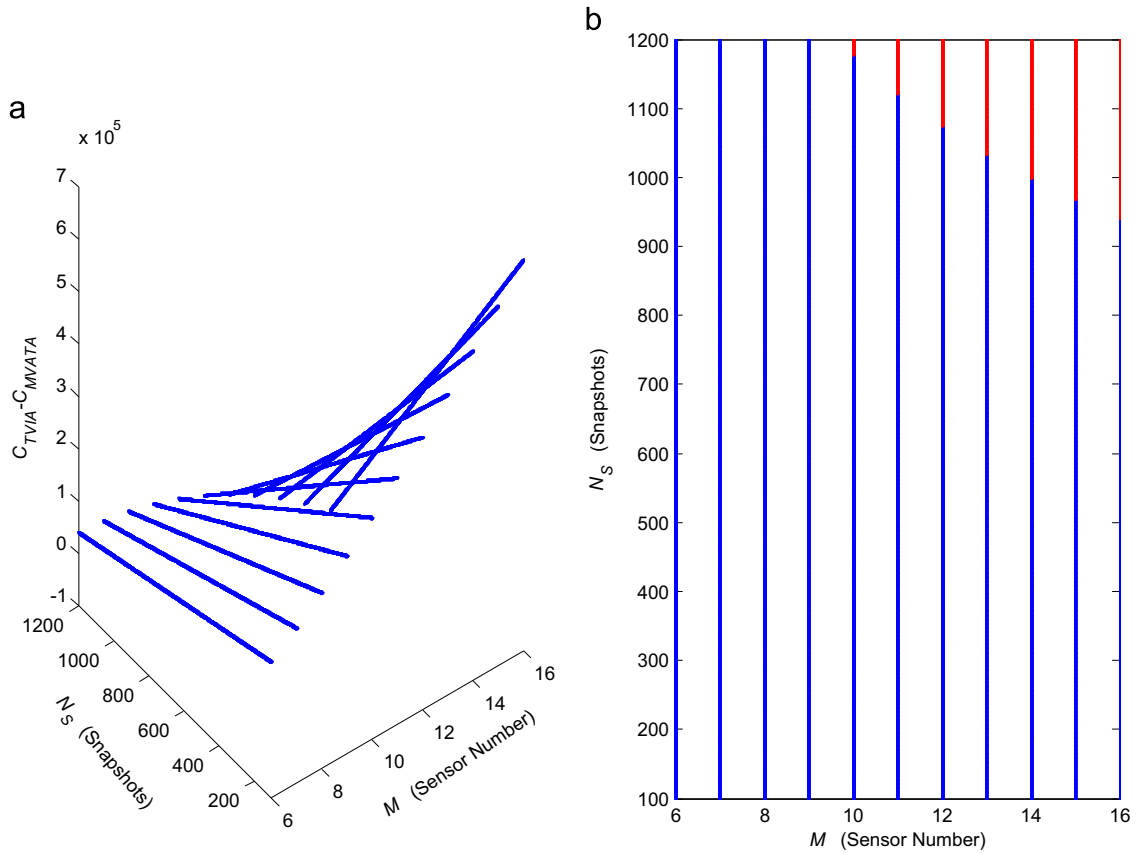


Fig. 4. Computational complexity.

then there exist two interpolation matrices \mathbf{B}_{k1} and \mathbf{B}_{k2} between the real and virtual subarrays that satisfy the following equation

$$\begin{cases} \mathbf{B}_{k1} \mathbf{A}_f = \mathbf{A}' \\ \mathbf{B}_{k2} \mathbf{A}_f = \mathbf{A}'' \end{cases} \quad (18)$$

$$\begin{cases} \mathbf{B}_{k1} \mathbf{a}_f(\theta_\alpha, \theta_\beta) = \mathbf{a}'(\theta_\alpha, \theta_\beta) \\ \mathbf{B}_{k2} \mathbf{a}_f(\theta_\alpha, \theta_\beta) = \mathbf{a}''(\theta_\alpha, \theta_\beta) \end{cases} \quad \theta_\alpha \in \Theta_\alpha, \quad \theta_\beta \in \Theta_\beta \quad (19)$$

Obviously, it is impossible to find two ideal \mathbf{B}_{k1} and \mathbf{B}_{k2} satisfy Eq. (18), (19). The accuracy of the interpolation is examined by calculating the ratios of the Frobenius norms [14]

Table 2
Computational complexity of the proposed MVATA.

Estimate the elevation and the azimuth by ESPRIT	MDN
a) $\mathbf{X}' = \mathbf{B}_{k1} \mathbf{X}$	$M^2 P$
b) $\mathbf{X}'' = \mathbf{B}_{k2} \mathbf{X}$	$M^2 P$
c) $\mathbf{R}_{YY} = E[\mathbf{Y}\mathbf{Y}^H]$	$(2M)^2(N_S) + 1$
d) $\mathbf{R}_{YY} = \mathbf{U}\Sigma\mathbf{U}^H$	$(2M)^3 + 2(2M)^2$
e) $\Psi = \text{pinv}(\mathbf{U}_{S1})\mathbf{U}_{S2}$	$\frac{2}{3}P^2 + MP^2$
f) $\text{SVD}(\Psi)$	$P^3 + 2P^2$
g) $\beta_p = \arccos\left\{\frac{\lambda}{2\pi d \sin \delta} \arccos\left(\frac{\text{abs}(D_p)}{2}\right)\right\} \frac{180^\circ}{\pi}$	$8P$
h) $\alpha_p = \arcsin\left(\frac{-\text{angle}(D_p)\lambda}{2\pi d \cos \delta \sin \beta_p}\right) \frac{180^\circ}{\pi}$	$8P$
Total MDN	
$M^2 P + M^2 P + (2M)^2(N_S) + 1 + (2M)^3 + 2(2M)^2 + \frac{2}{3}P^2 + MP^2 + P^3 + 2P^2 + 8P + 8P$	
$= 8M^3 + (4N_S + 2P + 8)M^2 + MP^2 + P^3 + \frac{8}{3}P^2 + 16P + 1$	

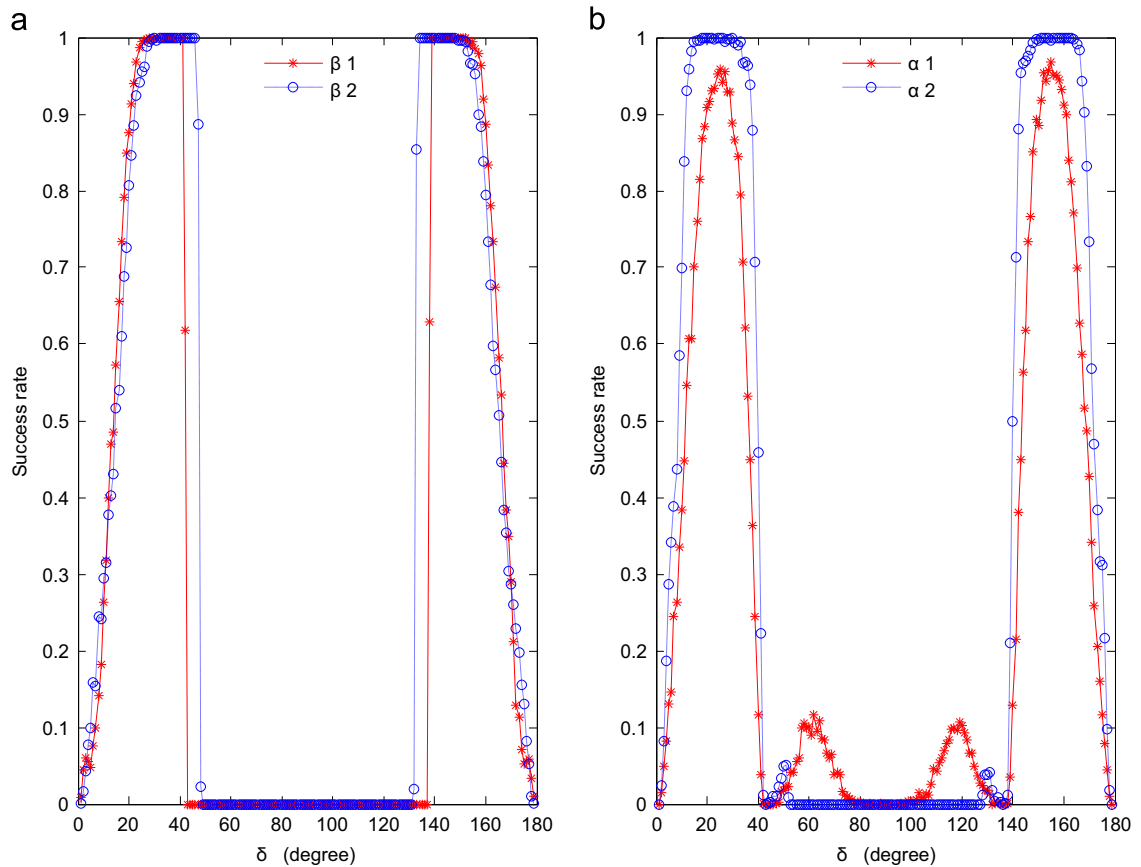


Fig. 5. DOA estimation success rate versus the direction angle.

$$\varepsilon' = \frac{\|\mathbf{B}_{k1}\mathbf{A}_f - \mathbf{A}'\|}{\|\mathbf{A}_f\|} \quad \text{and} \quad \varepsilon'' = \frac{\|\mathbf{B}_{k2}\mathbf{A}_f - \mathbf{A}''\|}{\|\mathbf{A}_f\|} \quad (20)$$

ε' and ε'' can examine the accuracy of the virtual array \mathbf{A}' and \mathbf{A}'' respectively. If both ε' and ε'' are small enough, for example, 0.001 [14], then \mathbf{B}_{k1} and \mathbf{B}_{k2} can be accepted. If these ratios are not sufficiently small, we can adjust the interpolation numbers J and I , and recalculate them. A stable and accurate method to solve the \mathbf{B}_{k1} and \mathbf{B}_{k2} is

described as follows: firstly we compute the singular value decomposition of \mathbf{A}_f as

$$\mathbf{A}_f = \mathbf{U}[\Sigma, 0][\mathbf{V}_1 \quad \mathbf{V}_2]^H \quad (21)$$

then \mathbf{B}_{k1} and \mathbf{B}_{k2} can be obtained by

$$\begin{aligned} \mathbf{B}_{k1} &= \mathbf{U}\Sigma^{-1}\mathbf{V}_1^H(\mathbf{A}')^H \\ \mathbf{B}_{k2} &= \mathbf{U}\Sigma^{-1}\mathbf{V}_1^H(\mathbf{A}'')^H \end{aligned} \quad (22)$$

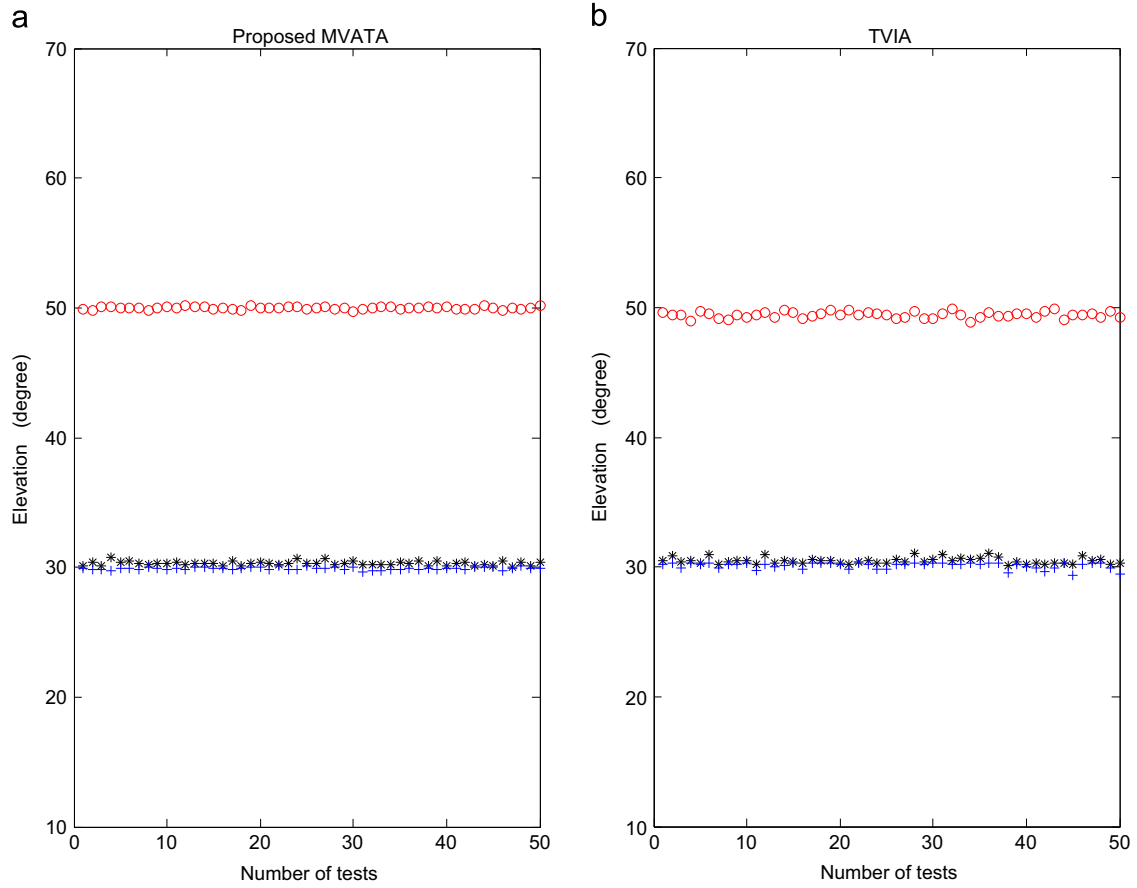


Fig. 6. Scatter plots of the estimated elevation angle.

Once \mathbf{B}_{k1} and \mathbf{B}_{k2} of real and virtual subarrays are derived by Eq. (22), the interpolation receiving data \mathbf{X}' and \mathbf{X}'' corresponding virtual subarray showed in Fig. 3 are computed by

$$\begin{aligned}\mathbf{X}' &= \mathbf{B}_{k1}\mathbf{X} = \mathbf{U}\mathbf{\Sigma}^{-1}\mathbf{V}_1^H(\mathbf{A}')^H\mathbf{A}\mathbf{S} + \mathbf{N}' \\ \mathbf{X}'' &= \mathbf{B}_{k2}\mathbf{X} = \mathbf{U}\mathbf{\Sigma}^{-1}\mathbf{V}_1^H(\mathbf{A}'')^H\mathbf{A}\mathbf{S} + \mathbf{N}''\end{aligned}\quad (23)$$

where \mathbf{A} is $M \times P$ array steering matrix. Considering the relative position of the three arrays, Eq. (23) can be further written as

$$\begin{aligned}\mathbf{X}' &= \mathbf{A}\Phi_1\mathbf{S} + \mathbf{N}' \\ \mathbf{X}'' &= \mathbf{A}\Phi_2\mathbf{S} + \mathbf{N}''\end{aligned}\quad (24)$$

where

$$\Phi_1 = \begin{bmatrix} e^{-j\frac{2\pi}{\lambda}(d \cos \delta \sin \alpha_1 \sin \beta_1 + d \sin \delta \cos \beta_1)} & & \\ & \ddots & \\ & & e^{-j\frac{2\pi}{\lambda}(d \cos \delta \sin \alpha_p \sin \beta_p + d \sin \delta \cos \beta_p)} \end{bmatrix}\quad (25)$$

$$\Phi_2 = \begin{bmatrix} e^{-j\frac{2\pi}{\lambda}(d \cos \delta \sin \alpha_1 \sin \beta_1 - d \sin \delta \cos \beta_1)} & & \\ & \ddots & \\ & & e^{-j\frac{2\pi}{\lambda}(d \cos \delta \sin \alpha_p \sin \beta_p - d \sin \delta \cos \beta_p)} \end{bmatrix}\quad (26)$$

The superposition of the two receiving arrays can be expressed as

$$\mathbf{X}_{12} = \mathbf{X}' + \mathbf{X}'' = \mathbf{A}_{12}\mathbf{S} + \mathbf{N}_{12} = \mathbf{A}\Phi_{12}\mathbf{S} + \mathbf{N}_{12}\quad (27)$$

where

$$\Phi_{12} = \Phi_1 + \Phi_2 = \begin{bmatrix} \ddots & & \\ 2 \cos(\frac{2\pi d \sin \delta}{\lambda} \cos \beta_p) e^{-j\frac{2\pi}{\lambda} d \cos \delta \sin \alpha_p \sin \beta_p} & & \\ & \ddots & \end{bmatrix}\quad (28)$$

\mathbf{X} and \mathbf{X}_{12} are combined in one matrix \mathbf{Y} of size $2M \times N_S$ as

$$\mathbf{Y} = \begin{bmatrix} \mathbf{X} \\ \mathbf{X}_{12} \end{bmatrix} = \mathbf{G}\mathbf{S} + \widehat{\mathbf{N}}\quad (29)$$

where

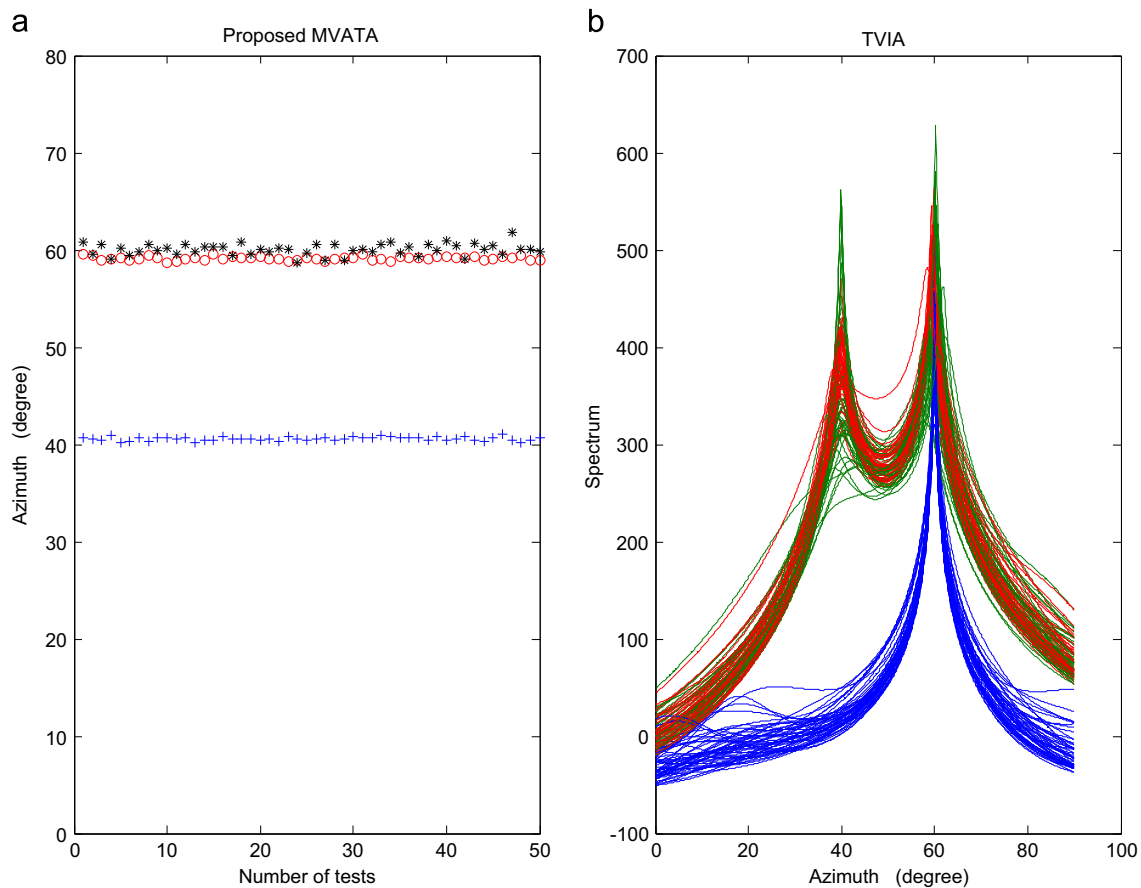


Fig. 7. Performance of estimated azimuth angle.

$$\mathbf{G} = \begin{bmatrix} \mathbf{A} \\ \mathbf{A}\Phi_{12} \end{bmatrix}, \quad \mathbf{N} = \begin{bmatrix} \mathbf{N} \\ \mathbf{N}_{12} \end{bmatrix} \quad (30)$$

Now the covariance matrix of the observed data is

$$\mathbf{R}_{\mathbf{Y}\mathbf{Y}} = E[\mathbf{Y}\mathbf{Y}^H] = \mathbf{G}\mathbf{R}_{\mathbf{S}\mathbf{S}}\mathbf{G}^H + \mathbf{R}_{\widehat{\mathbf{N}}\widehat{\mathbf{N}}} \quad (31)$$

where $\mathbf{R}_{\widehat{\mathbf{N}}\widehat{\mathbf{N}}} = E[\widehat{\mathbf{N}}\widehat{\mathbf{N}}^H]$ denotes the covariance matrix of the noise matrix $\widehat{\mathbf{N}}$. The estimate signal covariance matrix $\widehat{\mathbf{R}}_{\mathbf{Y}\mathbf{Y}}$ has $2M$ eigenvalues. We suppose $\mathbf{U}_{\mathbf{G}\mathbf{S}} = [\mathbf{v}_1, \mathbf{v}_2, \dots, \mathbf{v}_P]$ consists of the eigenvectors corresponding to P largest eigenvalues, and spans the signal subspace, and $\mathbf{U}_{\mathbf{G}\mathbf{N}} = [\mathbf{v}_{P+1}, \mathbf{v}_{P+2}, \dots, \mathbf{v}_{2M}]$ are the eigenvectors corresponding to the noise eigenvalues which span the noise subspace. It is clear $\mathbf{U}_{\mathbf{G}\mathbf{S}}$ has a dimension of $2M \times P$ and can be decomposed into two block matrices $\mathbf{U}_{\mathbf{S}1}$ and $\mathbf{U}_{\mathbf{S}2}$ as

$$\mathbf{U}_{\mathbf{G}\mathbf{S}} = \begin{bmatrix} \mathbf{U}_{\mathbf{S}1} \\ \mathbf{U}_{\mathbf{S}2} \end{bmatrix} \quad (32)$$

where $\mathbf{U}_{\mathbf{S}1}$ and $\mathbf{U}_{\mathbf{S}2}$ are termed as real and virtual subspaces, which both have a size of $M \times P$. It is easy to see that $\mathbf{U}_{\mathbf{G}\mathbf{S}}$ and \mathbf{G} span the same subspace. Therefore, [16] deduces

$$\mathbf{U}_{\mathbf{G}\mathbf{S}} = \mathbf{G}\mathbf{T} \quad (33)$$

here \mathbf{T} is a full-rank matrix. The shift invariance structure of the array implies that

$$\mathbf{U}_{\mathbf{G}\mathbf{S}} = \begin{bmatrix} \mathbf{U}_{\mathbf{S}1} \\ \mathbf{U}_{\mathbf{S}2} \end{bmatrix} = \begin{bmatrix} \mathbf{A}\mathbf{T} \\ \mathbf{A}\Phi_{12}\mathbf{T} \end{bmatrix} \quad (34)$$

$$\text{span}\{\mathbf{U}_{\mathbf{S}1}\} = \text{span}\{\mathbf{A}\} = \text{span}\{\mathbf{U}_{\mathbf{S}2}\} \quad (35)$$

where span represents the column linear span. Applying (27) and (34) we get

$$\mathbf{U}_{\mathbf{S}2} = \mathbf{A}(\mathbf{T}\mathbf{T}^{-1})\Phi_{12}\mathbf{T} = \mathbf{U}_{\mathbf{S}1}\mathbf{T}^{-1}\Phi_{12}\mathbf{T} = \mathbf{U}_{\mathbf{S}1}\Psi \quad (36)$$

$$\Phi_{12} = \mathbf{T}\Psi\mathbf{T}^{-1} \quad (37)$$

Since Ψ and Φ_{12} are related via a similarity transformation, both have the same eigenvalues, i.e., the elements in the diagonal of Ψ are same as the eigenvalues of Φ_{12} . That means, Φ_{12} can be obtained via an eigenvalue decomposition (EVD) of Ψ , Ψ can be obtained as

$$\Psi = \text{pinv}(\mathbf{U}_{\mathbf{S}1})\mathbf{U}_{\mathbf{S}2} \quad (38)$$

where pinv denotes Moore Penrose Inverse. The 2D DOA can be estimated via

$$\beta_p = \arccos\left\{\frac{\lambda}{2\pi d \sin \delta} \arccos\left(\frac{\text{abs}(D_p)}{2}\right)\right\} \frac{180^\circ}{\pi} \quad (39)$$

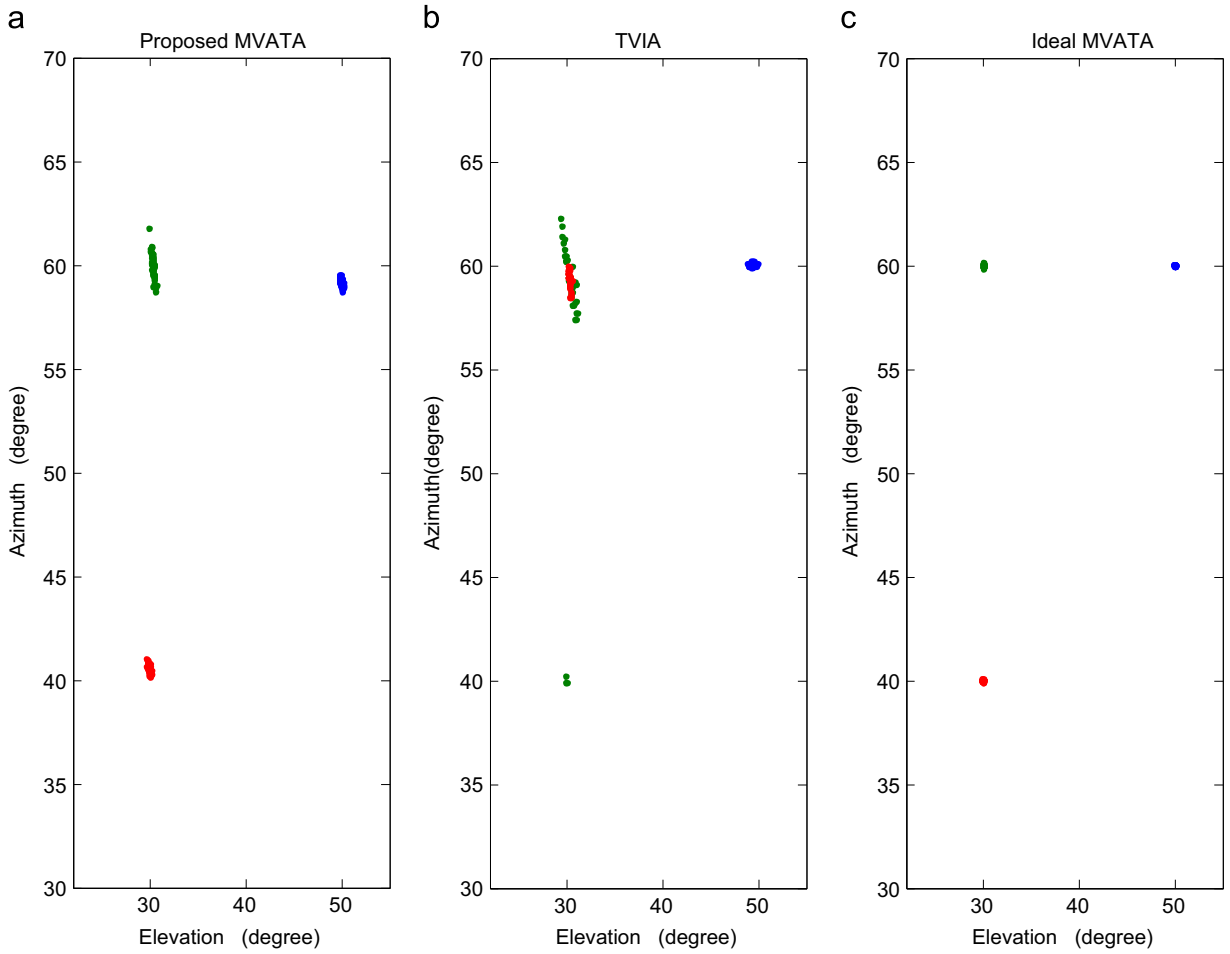


Fig. 8. Scatter plots of the azimuth angle versus the elevation angle.

$$\alpha_p = \arcsin\left(\frac{-\angle(D_p)\lambda}{2\pi d \cos\delta \sin\beta_p}\right) \frac{180^\circ}{\pi} \quad (40)$$

where D_p , $p = 1, 2, \dots, P$ are the eigenvalues of the matrix Ψ .

4. Computational complexity analysis

In this section, we carefully analyze the computational complexity of TVIA and the proposed MVATA. Let MDN denote number of multiplications and divisions and N_S represent number of snapshots. Γ in Table 1 denotes the number of searches conducted along the DOA axis, it is set usually much bigger than M in order to obtain an accurate DOA estimation, Fig. 4 shows the difference of computational complexity, where C_{TVIA} and C_{MVATA} represent the computational complexity of TVIA and proposed MVATA. Let the number of source $P = 1$, the number of searches conducted along the azimuth axis be 1800, these two parameters are same as the experiment 3 and 4. The simulation results demonstrate that in most cases the difference of $C_{TVIA} - C_{MVATA}$ is much larger than zero, which indicates our computational complexity is significantly lower than TVIA. In Fig. 4(b), the red curves

correspond to the cases which the computational complexity of proposed larger than TVIA, the blue curves corresponding the opposite. It can be seen our algorithm possesses the advantage in the small snapshots Table 2.

5. Experimental results

In this section, five experiments are presented to show the performances improvement of proposed MVATA compared with the TVIA. A UCA of radius $R = 0.6533\lambda$ with $M = 8$ is employed, and the search step size of TVIA is set to be 0.1° in all experiments. N_S denotes the number of snapshots in the simulations. The signals and noise are assumed to be stationary, zero mean, and uncorrelated Gaussian random processes. Noise is both spatially and temporally white. SNR is defined as the ratio of the received source power versus the noise power at the sensor.

5.1. Experiment 1

As mentioned above, parameter δ represents the direction angles of the two interpolated virtual arrays. We analyze the estimation success rate versus different direction angle δ , 700

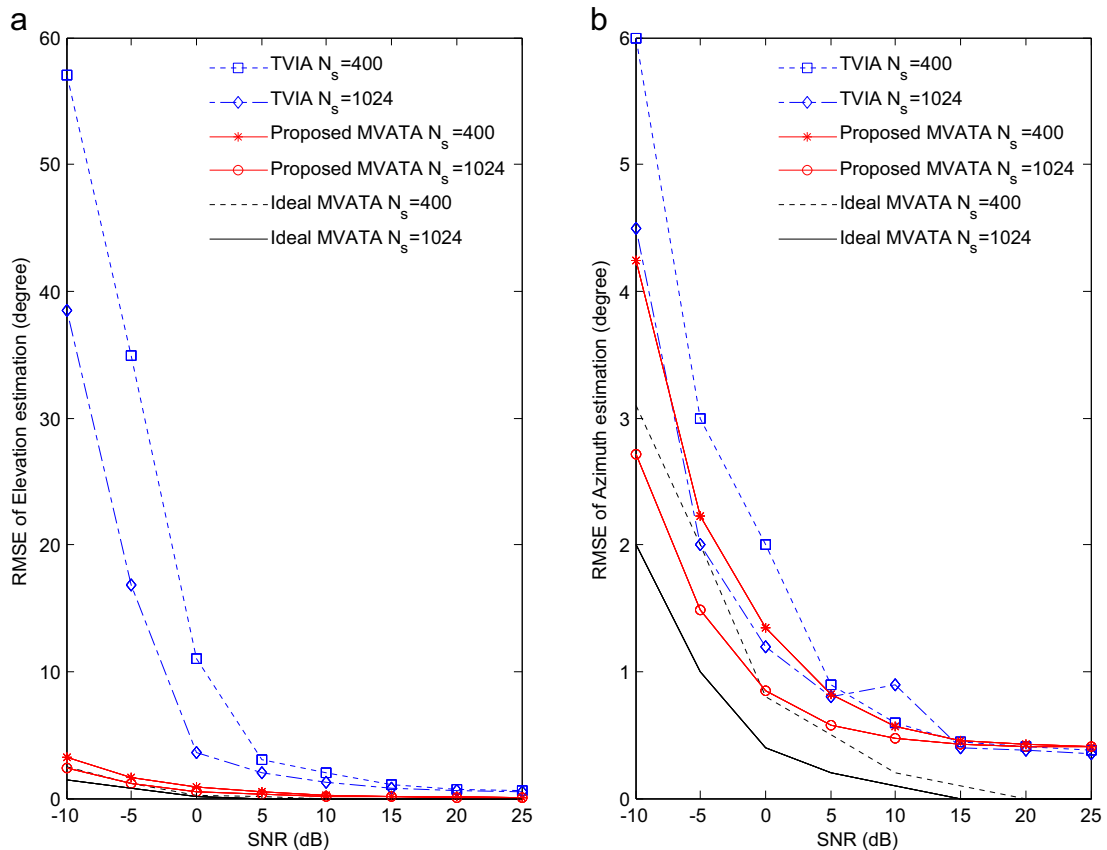


Fig. 9. The RMSE of 2D DOA versus SNR.

Monte Carlo experiments are carried out using a set of δ , $\delta \in (0^\circ, 90^\circ) \cup (90^\circ, 180^\circ)$. Suppose that two uncorrelated narrowband signals impinge on the array from $\Theta_\beta \in [20^\circ, 50^\circ]$ and $(\beta_2 = 60^\circ, \alpha_2 = 35^\circ)$ respectively. The SNR is set as 20 dB, 1024 snapshots are taken, the interpolation sectors are chosen as $\Theta_\alpha \in [25^\circ, 50^\circ]$ and $\Theta_\beta \in [35^\circ, 65^\circ]$, the interpolation step $\Delta\phi$ is 1° . Fig. 5 shows the DOA estimation success rate of the proposed MVATA versus the direction angle δ . According to the Eq. (28), the angle α_p and β_p can be estimated at the same time only if $\delta \neq 0^\circ, 90^\circ$, and 180° . This also means that the centers of the arrays \mathbf{A}, \mathbf{A}' and \mathbf{A}'' cannot be collinear. When $\delta = 0^\circ, 90^\circ$, and 180° , the proposed MVATA will become single direction virtual interpolation algorithm. The Fig. 5 shows the proposed MVATA is failure at this time. There is an interesting phenomena that the proposed MVATA has high success rate while the direction angle $\delta \in (15^\circ, 35^\circ) \cup (145^\circ, 165^\circ)$, we find that the $\delta \in (15^\circ, 35^\circ)$ and $\delta \in (145^\circ, 165^\circ)$ both corresponding the same scenario because of symmetry. Under this scenario, the center distance between two virtual circle arrays is within $(0.29\lambda, 0.57\lambda)$.

5.2. Experiment 2

The second experiment shows the 2D DOA estimation performance of TVIA with the proposed MVATA. Suppose that three uncorrelated narrowband signals impinge on the array from $(\beta_1 = 30^\circ, \alpha_1 = 60^\circ)$, $(\beta_2 = 30^\circ, \alpha_2 = 40^\circ)$ and $(\beta_3 = 50^\circ, \alpha_3 = 60^\circ)$, respectively. The SNR is set as 35 dB,

1024 snapshots are taken, the interpolation sectors are chosen as $\Theta_\beta \in [25^\circ, 50^\circ]$ and $\Theta_\alpha \in [35^\circ, 65^\circ]$, the direction angle δ equals 25° , the interpolation step $\Delta\phi$ is 1° , and 50 independent measurements are carried out. It can be seen from Figs. 6, 7 and 8 that the proposed MVATA has much better angle estimation performance than the TVIA. It is important to point out that the proposed MVATA can easily distinguish signals with the same elevation but different azimuths. On the contrary, the TVIA is difficult to distinguish them in this case. The reason is that the proposed MVATA obtained the azimuth via Eq. (40) and can obtain a closed form solution, while TVIA obtain azimuth through spectrum peak search with a fixed elevation. Hence the azimuths will be paired incorrectly sometimes, i.e. if signals with the same elevation but different azimuths, they cannot be distinguished sometimes. Suppose it is possible to find ideal \mathbf{B}_{k1} and \mathbf{B}_{k2} to satisfy Eq. (18) $\mathbf{B}_{k1}\mathbf{A}_f = \mathbf{A}'$ $\mathbf{B}_{k2}\mathbf{A}_f = \mathbf{A}''$, the proposed MVATA can achieve optimal performance, Fig. 8(c) shows the experimental results of the proposed MVATA in such a condition.

5.3. Experiment 3

Let 500 Monte Carlo experiments be carried out with different SNR (from -10 dB to 25 dB), we select the number of snapshots as 400 and 1024. The root mean squared error (RMSE) [17] criterion is employed to compare the DOA estimation results of different algorithms,

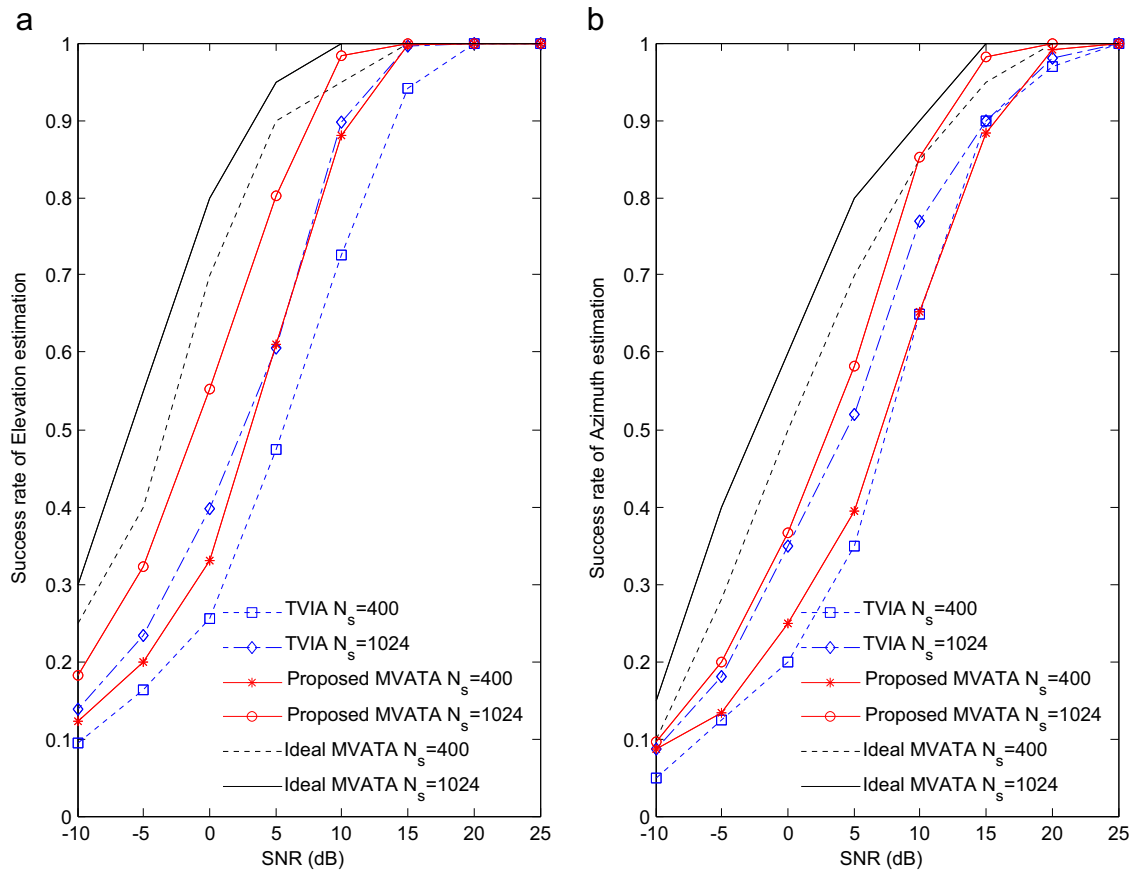


Fig. 10. The success rate of 2D DOA versus SNR.

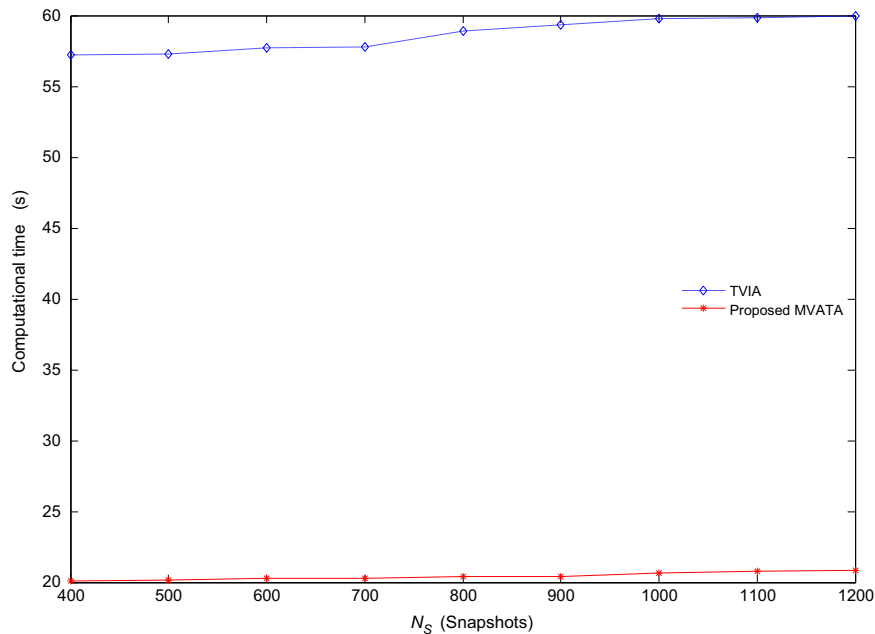


Fig. 11. Computational time versus snapshots.

and it is calculated as

$$\text{RMSE} = \sqrt{\frac{1}{N} \sum_{n=1}^N \left[\frac{1}{P} \sum_{p=1}^P (\hat{\theta}_p(n) - \theta_p)^2 \right]} \quad (\text{degree}) \quad (41)$$

where N is the number of the Monte Carlo experiments, P is the number of signals, θ_p is the p th DOA and $\hat{\theta}_p$ denotes the p th estimated DOA in the n th Monte Carlo experiment. Suppose that a narrowband signal impinges on the array from $(\beta_1 = 30^\circ, \alpha_1 = 30^\circ)$. The interpolation sectors are chosen as $\Theta_\beta \in [20^\circ, 40^\circ]$ and $\Theta_\alpha \in [20^\circ, 40^\circ]$, the direction angle δ equals 25° , and the interpolation step $\Delta\phi$ adopts 1° . Fig. 9 shows RMSE of the proposed MVATA and TVIA. The results demonstrate that the performances of proposed MVATA are more accurate than TVIA especially in the cases of low SNR and small snapshots.

5.4. Experiment 4

500 Monte Carlo experiments are carried out with different SNR (from -10 dB to 25 dB), the number of snapshots are selected as 400 and 1024 respectively. This experiment compares the 2D DOA estimation success rate of the proposed MVATA with the TVIA versus SNR. Suppose that a narrowband signal impinges on the array from $(\beta_1 = 30^\circ, \alpha_1 = 30^\circ)$. The interpolation sectors are chosen as $\Theta_\beta \in [20^\circ, 40^\circ]$ and $\Theta_\alpha \in [20^\circ, 40^\circ]$, the direction angle δ equals 25° , and the interpolation step $\Delta\phi$ adopts 1° . Fig. 10 shows success rate performance of the proposed MVATA and TVIA. The proposed MVATA still offers a better performance than the TVIA in low SNR and small snapshots.

5.5. Experiment 5

In this experiment, we compare the computational cost of the proposed MVATA with TVIA. Suppose that two uncorrelated narrowband signals impinge on the array from $\Theta_\beta \in [20^\circ, 50^\circ]$ and $(\beta_2 = 60^\circ, \alpha_2 = 35^\circ)$ respectively. The interpolation sectors are chosen as $\Theta_\beta \in [20^\circ, 50^\circ]$ and $\Theta_\alpha \in [35^\circ, 65^\circ]$, the direction angle δ equals 25° , and the interpolation step $\Delta\phi$ adopts 1° . 500 Monte Carlo experiments are carried out using a set of different snapshot levels (from 400 to 1200), SNR is set as 20 dB, the experimental results as shown in Fig. 11. Fig. 11 shows the computational time of the proposed MVATA and the TVIA. Under the same calculation condition, the computational time of the proposed MVATA is much smaller than the TVIA.

6. Conclusions

In order to improve the performance of virtual interpolation algorithm in finite snapshots and low SNR, a new algorithm termed MVATA for 2D DOA estimation is proposed. MVATA can derive the azimuth and elevation by using only once ESPRIT. It can be applied to arbitrary structure array and the estimated 2D angles can be paired automatically. Moreover, two dimension angles which have the same azimuth or elevation angle can also be distinguished. Compared with the TVIA, theoretical

calculation and time-consuming statistics show that the proposed MVATA has the advantage of low computational complexity. The experiments of success rates and RMSE versus SNR, the scatter plots of the estimated azimuth and elevation angle, and the computational time versus snapshots are presented. Simulations show the proposed algorithm possesses significantly performance improvement especially in low SNR and small snapshots.

Acknowledgments

The authors would like to thank very much the Handling Editor Jean Pierre Delmas, Journal Manager Chitra and the anonymous reviewers for their valuable comments and suggestions that have significantly improved the manuscript.

This work was supported by the National Natural Science Foundation of China under Grants 61373177, 61271293, 61272461 and 61572402; Natural Science Basic Research Plan in Shaanxi Province of China under Grant 2013JM8008.

References

- [1] F. Wang, X.W. Cui, M.Q. Lu, et al., Decoupled 2D direction-of-arrival estimation based on sparse signal reconstruction, *EURASIP J. Adv. Signal Process.* 7 (2015).
- [2] R.O. Schmidt, Multiple emitter location and signal parameter estimation, *IEEE Trans. Antennas Propag.* 34 (3) (1986) 276–280.
- [3] R. Roy, ESPRIT-estimation of signal parameters via rotational invariance techniques, *IEEE Trans. Acoustics Speech Signal Process.* 37 (7) (1989) 984–995.
- [4] Y.S. Wei, X. Guo, Pair-matching method by signal covariance matrices for 2D DOA estimation, *IEEE Antennas Wireless Propag. Lett.* 13 (6) (2014) 1199–1202.
- [5] Q. Li, Y. Jiang, X. Diao, A DOA estimation algorithm of virtual array based on beamforming, in: *Proceedings of the IEEE International Conference on Electrical and Control Engineering (ICECE)*, 2011, pp. 945–948.
- [6] A.M. Marco, Marinho, João Paulo, C. L. da Costa, Unscented transformation based array interpolation, *IEEE Conference Publications*, 2015, pp. 2819–2823.
- [7] J. He, M.O. Ahmad, M.N.S. Swamy, Extended-aperture angle-range estimation of multiple Fresnel-region sources with a linear tripole array using cumulants, *Signal Process.* 92 (4), pp. 939–953.
- [8] W. Feng, W.P. Zhu, M.N.S. Swamy, Spatial extrapolation-based blind DOA estimation approach for closely spaced sources, *IEEE Trans. Aerosp. Electron. Syst.* 46 (2) (2010) 569–582.
- [9] H. Chen, C.P. Hou, Q. Wang, Cumulants-based toeplitz matrices reconstruction method for 2-D coherent DOA estimation, *IEEE J. Mag.* (2014) 2824–2832.
- [10] T. P. Bronez, Sector interpolation of non-uniform arrays for efficient high resolution bearing estimation, in: *Proceedings of the International Conference on Acoustics, Speech, and Signal Processing*, 1988, pp. 2885–2888.
- [11] B. Friedlander, The root-MUSIC algorithm for direction finding with interpolated arrays, *Signal Process.* 30 (1) (1993) 15–29.
- [12] P. Yang, F. Yang, Z.P. Nie, et al., Robust adaptive beamformer using interpolation technique for conformal antenna array, *Prog. Electromag. Res. B* 23 (2010) 215–228.
- [13] X.J. Sun, Circle array receiving signal 2D DOA separable estimation based on twice virtual interpolations, *J. Electron. Inf. Technol.* 30 (8) (2008) 1890–1892.
- [14] P. Yang, F. Yang, Z.P. Nie, et al., Doa estimation with sub-array divided technique and interpolated esprit algorithm on a cylindrical conformal array antenna, *Progress in Electromagnetic, Prog. Electromag. Res.* 103 (4) (2010) 201–216.

- [15] L. Huang, H.C. So, Source enumeration via MDL criterion based on linear shrinkage estimation of noise subspace covariance matrix, *IEEE Trans. Signal Process.* 61 (19) (2013) 4806–4821.
- [16] D.Z. Feng, X.D. Zhang, Z. Bao, A neural network learning for adaptively extracting cross-correlation features between two high-dimensional data streams, *IEEE Trans. Neural Netw.* 15 (6) (2004) 1541–1554.
- [17] S. Zhao, T. Saluev, D.L. Jones, Underdetermined direction of arrival estimation using acoustic vector sensor, *Signal Process.* 100 (7) (2014) 160–168.